Cardiovascular Pathology 22 (2013) 58–64

Contents lists available at SciVerse ScienceDirect

Cardiovascular Pathology

Original Article

The clinical significance of the atrial subendocardial smooth muscle layer and cardiac myofibroblasts in human atrial tissue with valvular atrial fibrillation

Jae Hyung Park [a], Hui-Nam Pak [a,*], Sak Lee [a], Han Ki Park [a], Jeong-Wook Seo [b], Byung-Chul Chang [a,*]

[a] Yonsei University Health System, Seoul, Republic of Korea
[b] Department of Pathology, Seoul National University College of Medicine, Seoul, Republic of Korea

ARTICLE INFO

Article history:
Received 18 February 2012
Received in revised form 14 April 2012
Accepted 3 May 2012

Keywords:
Atrial fibrillation
Myofibroblast
Subendocardial smooth muscle layer

ABSTRACT

Background: The existence of myofibroblasts (MFBs) and the role of subendocardial smooth muscle (SSM) layer of human atrial tissue in atrial fibrillation (AF) have not yet been elucidated. We hypothesized that the SSM layer and MFB play some roles in atrial structural remodeling and maintenance of valvular AF in patients who undergo cardiac surgery.

Methods: We analyzed immunohistochemical staining of left atrial (LA) appendage tissues taken from 17 patients with AF and 15 patients remaining in sinus rhythm (SR) who underwent cardiac surgery (male 50.0%, 54.1±14.2 years old, valve surgery 87.5%). SSM was quantified by α-smooth muscle actin (α-SMA) stain excluding vascular structure. MFB was defined as α-SMA+ cells with disorganized Connexin 43-positive gap junctions in Sirius red-positive fibrotic area.

Results: The SSM layer of atrium was significantly thicker in patients with AF than in those with SR (P=.0091). Patients with SSM layer ≥14 μm had a larger LA size (P=.0006) and greater fibrotic area (P=.0094) than those patients whose SSM layer <14 μm. MFBs were found in 7 of 17 (41.2%) patients with AF and 2 of 15 (13.3%) in SR group (P=.0456) in SSM area, colocalized with Periodic Acid-Schiff (PAS) stain-positive glycogen storage cells (95.5%).

Conclusion: SSM layer was closely related to the existence of AF, degrees of atrial remodeling, and fibrosis in patients who underwent open heart surgery. We found that MFB does exist in SSM layer of human atrial tissue co-localized with PAS-positive cells.

1. Introduction

It has been shown that structural remodeling related to aging and heart disease, such as increased myocardial fibrosis, plays an important role in the maintenance mechanism of atrial fibrillation (AF) [1,2]. The integrity of interstitial matrix tissue is adversely affected by a large number of cardiac diseases, ranging from volume and/or pressure overload to overt heart failure. Under pathological conditions, complex reactions involving changes in extracellular matrix production, cell proliferation, and cell death cause structural remodeling, thus compromising the mechanical function and predisposing the heart to arrhythmias [3].Cardiac fibroblasts are essential for the formation of a normal myocardial wall, in particular in the production of parts of the collagen-rich matrix of the heart. Myofibroblasts (MFBs) have also been found in a diseased adult heart [4]. MFBs were found, for example, in a hypertensive heart and infarcted myocardium, where they are involved in the establishment of fibrosis and the formation of the infarct scar [4]. This cell type, which plays a central role in wound healing in general, is characterized by de novo expression of α-smooth muscle actin (α-SMA) [5] and disorganized patterns of connexin (Cx) associated with fibrosis [5,6]. However, MFB has not yet been proven to exist in the human atrial tissue, and it is not clear whether MFB plays any role in the atrial remodeling process in patients with AF. In this study, we hypothesized that the degree of subendocardial remodeling of atrial tissue is significantly different in patients with AF compared to those remaining in sinus rhythm (SR), and MFB exists in the human atrial tissue. The purpose of this study was to evaluate the histology and cellular characteristics of subendocardial the smooth muscle (SSM) layer, the appearance of MFBs, and their relationship to glycogen storage cells in human atrial appendage tissues taken from patients with varying degrees of atrial structural remodeling and rhythm status.

2. Methods

2.1. Patient selection

The study protocol was approved by the institutional review board of Severance Cardiovascular Hospital, Yonsei University Health

Disclosure information: nothing to disclose.

* Corresponding authors. Hui-Nam Pak, MD, PhD, is to be contacted at 250 Seungsanno, Seodaemun-gu, Seoul, Republic of Korea 120-752. Tel.: +82 2 2228 8459; fax: +82 2 393 2041. Byung-Chul Chang, MD, PhD 250 Seungsanno, Seodaemun-gu, Seoul, Republic of Korea 120-752. Tel.: +82 2 2228 8200; fax: +82 2 393 2041.
E-mail addresses: hnpak@yuhs.ac (H.-N. Pak), bcchang@yuhs.ac (B.-C. Chang).

1054-8807/$ – see front matter.
doi:10.1016/j.carpath.2012.05.001

System. All patients provided written informed consent. The study prospectively enrolled 32 patients (mean age 54.1±14.2 years, 50% male), who underwent open heart surgery (Table 1). Among them, 29 patients underwent valve surgery ($n=29$, 24 mitral valve surgery), and the remaining three patients underwent repair surgeries for atrial septal defect (ASD) and ventricular septal defect (VSD), and myomectomy for obstructive hypertrophic cardiomyopathy, each. Among them, 17 patients had AF, and 15 patients were in SR. Comprehensive transthoracic echocardiography was performed using commercially available devices (Sonos 5500; Philips Medical System, Andover, MA, USA, or Vivid 7; GE Vingmed Ultrasound, Horten, Norway). Standard M-mode, two-dimensional and Doppler images were acquired in parasternal and apical views. Left atrial (LA) anterior-posterior diameter was measured, and left ventricular (LV) end-diastolic dimension (LVEDD), LV end-systolic dimension (LVESD), and LV ejection fraction (EF) were calculated from two-dimensional images using the modified Quinones method. Early mitral inflow peak velocity (E) was measured using the pulsed-wave Doppler method by placing a sample volume at the opening level of the mitral valve leaflet tips. The tissue Doppler-derived diastolic mitral annular velocity (E′) and peak systolic mitral annular velocity (S′) were measured from the septal corner of the mitral annulus in the apical four-chamber view. Specimens of full wall thickness were excised from the LA appendage. All myocardial specimens were fixed in 70% alcohol and 10% formalin solution—immediately after the excision.

2.2. Immunohistochemical studies

Multiple 5-μm-thick serial sections were used. Sirius red stains were used to determine the presence and the degree of fibrosis. Periodic Acid-Schiff (PAS) staining was performed to assess the intracellular glycogen content. Immunohistochemical staining was performed using an avidin–biotin peroxidase system (Dako). Paraffin-embedded tissue sections were deparaffinized then washed with phosphate-buffered saline (PBS). A hydrogen peroxidase block (Dako, Carpenteria, CA, USA) was placed on the sections for 10 min, and the slides were washed in PBS. A protein block (Dako) was placed on the sections for 30 min. Slides were then incubated with primary antibodies for 90 min at room temperature (approx. 25°C). Antibodies for α-SMA (1:500 dilution, rabbit antihuman polyclonal; Abcam) were used to stain smooth muscle, while antibodies for Cx43 (1:500 dilution, rabbit anti Cx43; Sigma, C6219) were used to stain the morphology and structure of gap junctions. Some sections were double stained for α-SMA and Cx43. After incubation, the slides were washed in PBS, and the appropriate secondary antibody (Dako) was placed on the sections for 30 min. The sections were again washed in PBS, and the appropriate chromagen was added to each specimen. Smooth mucle cells and gap junctions were stained brown with 3,3′-diaminobenzidine (DAB). Cell nuclei were marked by placement of the specimens in hematoxyline (Merk) for 1 min. Specimens were then dehydrated in alcohol, mounted, and examined with light microscopy. The DAB stains were examined with light microscopy and virtual microscopy. The histopathological slides were analyzed using a computer-assisted morphometric analysis system (Image-Pro Plus 6.0).

2.3. Analysis of the SSM layer and MFB

The virtual microscopic images were selected and analyzed by a single investigator who was blinded to the clinical information of

Table 1
Clinical characteristics of the 32 patients enrolled in the study

	No.	Age	Sex	Undergoing diseases	Operation name	BMI	LA size	EF	E/E′	LVEDD	LVESD
AF	1	60	M	MS	MVR	26	76	58		58	42
	2	63	F	MS, TR, DM	MVR, TA	14	41	73		41	25
	3	74	F	MR (MVP)	MV repair	19	66	74	20	62	37
	4	60	F	MS, AS	DVR	24	68	61		57	40
	5	73	F	MS, DM, Hypertension	MVR	24	65	68		45	29
	6	51	M	MS, AS	Redo MVR	23	77	63		60	41
	7	73	M	MR, TR	MV repair	22	62	35	22	68	57
	8	47	M	MS, CAD	DVR	22	59	69		58	37
	9	67	F	MS, CAD, DM	MVR	24	60	56		49	36
	10	63	F	MS	MVR	26	58	71		43	27
	11	58	F	MR, TR, Hypertension	MV repair, TA	20	63	57	24	62	45
	12	35	M	MS, TR	MVR, TA	20	57	48		57	43
	13	62	M	MS, AR	DVR	25	79	52		58	40
	14	52	F	MS, TR	MVR, TA	25	55	62		42	29
	15	61	F	MR (MVP), ASD	MV repair, ASD closure	18	54	84	15	45	23
	16	67	F	MS, TR	MVR, TA	21	88	70		57	36
	17	67	M	MR	MV repair	21	66	45		54	42
						22.0±3.2	64.4±11.1	61.5±12.2	20.3±3.9	53.9±8.1	37.0±8.5
SR	1	31	M	ASR	AVR	22	48	36		71	57
	2	63	M	AR, CAD, Hypertension	AVR, CABG	20	43	63	11	70	48
	3	76	F	MSR, AR	MV repair	20	47	60	23	62	44
	4	54	M	MS, s/p Stroke	MVR	23	46	68		45	29
	5	35	F	MS	MVR	18	41	55		46	34
	6	52	F	AR, CAD	AVR	19	26	48	7	81	61
	7	62	M	AS, CRF, CAD, DM, Hypertension	AVR, CABG	23	53	31	50	64	53
	#8	51	M	MR(MVP)	MV repair	24	52	59	11	66	47
	#9	32	M	HCM	Myomectomy of LVOTO	20	32	61	15	53	33
	#10	50	F	MR	MVR	24	45	67		52	34
	#11	39	M	MS, TR	MVR, TA	21	66	51		57	42
	#12	38	F	MR (MVP), infective endocarditis	MVR	27	42	66	8	59	39
	#13	53	M	MS	MVR	28	52	74	21	52	31
	#14	19	M	VSD	VSD patch repair	20		64		49	32
	#15	43	F	ASD	ASD patch repair	22		60		47	32
						22.1±2.8	45.6±9.9	57.5±11.8	18.3±14.1	58.3±10.6	41.1±10.2

AR, aortic regurgitation; AS, aortic stenosis; ASR, aortic stenosis with regurgitation; AVR, aortic valve replacement; CABG, coronary artery bypass graft; CAD, coronary artery disease; CHF ,congestive heart failure; CRF, chronic renal failure; DM, diabetes mellitus; DVR, double valve replacement; HCM, hypertrophic cardiomyopathy; MR, mitral regurgitation; MS, mitral stenosis; MVR, mitral valve replacement; TA, tricuspid annuloplasty; TR, tricuspid regurgitation.

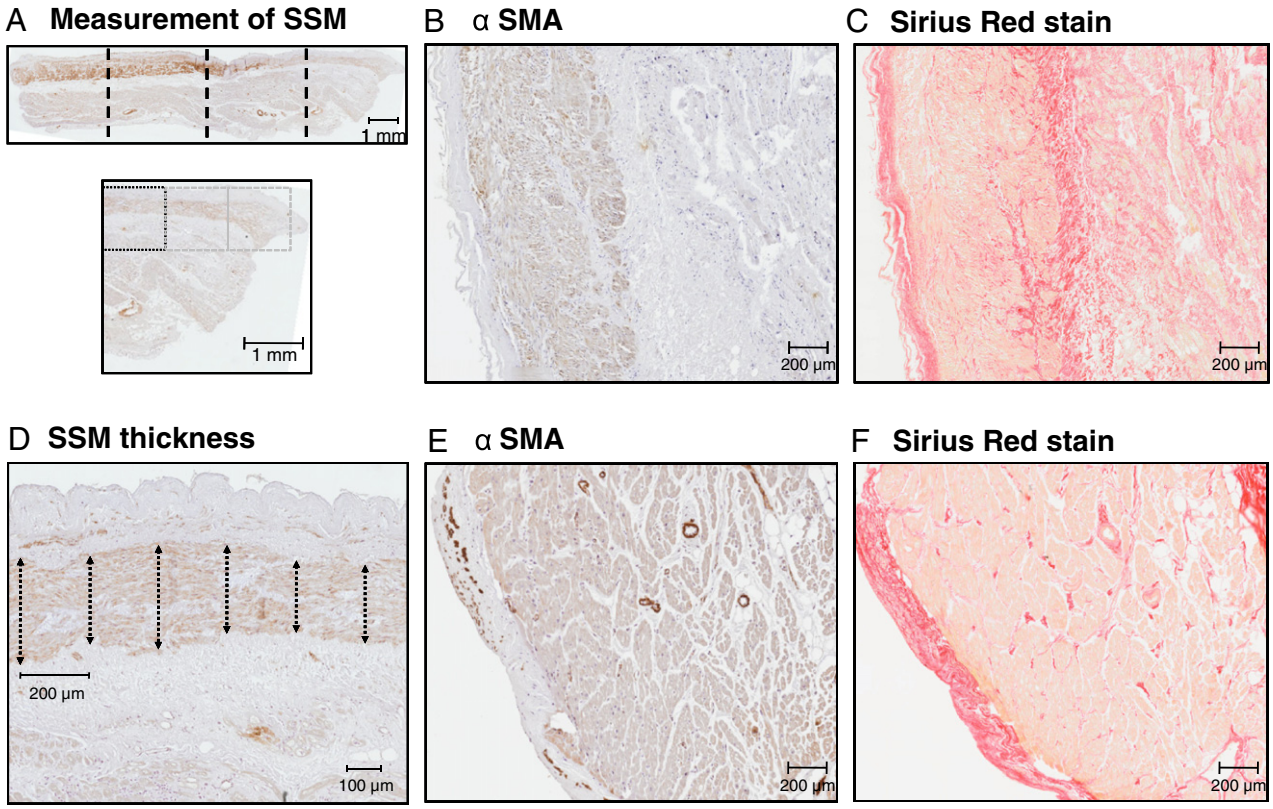

Fig. 1. We selected microscopic fields at four different sites (A) in each quadrant for the quantification of immunohistochemical staining. Smooth muscle thickness was measured every 200 μm (D). In patients with AF, the SSM was significantly thicker (B and E), and the fibrotic area was significantly larger (C and F) than in those in SR.

histological slides using a consistent method. To quantify the histologic evaluation, we generated 640virtual microscopic images (Olyvia; Olympus, Tokyo, Japan)of four regions from each of 32 slides with 5different stains (Masson's trichrome, Sirius red, and PAS stains, and immunostainings for α-SMA or Cx43). Then, virtual histology was divided into four parts for digital quantification and analyzed whole length of subendocardial layer (Image Pro, Media Cybernetics., Silver Spring, MD, USA) (Fig. 1A). In the virtual histology, the SSM area was identified as α-SMA immunohistostaining-positive structures between endocardium and myocardium, stained brown (RGB values: red 22–125, green 4–77, and blue 4–55), excluding perivascular smooth muscle. In the endocardium, we measured the thickness of endocardium and SSM layer every 200 μm along the endocardial surface (Fig. 1D). The gap junctions were identified by Cx43 immunostaining, and MFBs appeared to show scattered patterns of Cx43-positive structure on the SSM area with fibrosis (Fig. 2). The percent areas of fibrosis were quantified with Sirius red staining utilizing the Image Pro software. Therefore, our definition of MFB was the cells stained with α-SMA expressing disorganized patterns of Cx43 in the fibrotic subendocardium in accordance with Rohr's description [7]. We evaluated the colocalization percentage of MFB with PAS-positive glycogen storage cells.

2.4. Data analysis

Data are expressed as mean±S.D. We compared the thickness of SSM layer, fibrotic area, and the number of MFB between AF and SR patient groups. We also compared the clinical characteristics of the patients divided according to the median value of their SSM layer. Colocalization of MFBs and glycogen storage cells was also evaluated. The statistical significance of these comparisons was assessed using the Student's t and analysis of variance tests. $P<.05$ was considered statistically significant.

3. Results

3.1. Thicker SSM layer in atrial tissue with AF

Table 2 summarizes the comparisons of clinical, image, and histologic characteristics of atrial tissues in patients with SR and AF. In the AF group, the age of the patients was significantly higher ($P=.0003$), body surface area was smaller ($P=.0301$), and the proportion of mitral valve disease was higher (100% vs. 58.8%, $P=.0010$) than those remaining in SR. Although the duration of AF reflects the degree of structural remodeling of AF, most of patients could not recall the symptom onset of their longstanding persistent or permanent AF because it was hard to differentiate from symptoms associated with structural heart disease. The echocardiographically measured LA size ($P<.0001$) and volume index ($P=.0024$) were significantly greater in the AF group than in the SR group. For the histological analyses, SSM was quantified with α-SMA immunostaining, and the area of subendocardial fibrosis was evaluated with Sirius red staining (Fig. 1). We analyzed the thickness of SSM every 200 μm along the endocardial surface of 122 slides of α-SMA immunostaining. Both the percent area ($P=.0137$) and the thickness ($P=.0091$) of SSM were significantly higher and thicker in patients with AF than whose remained in SR (Fig. 1B and E). Endocardial thickness itself was also greater in AF group than in SR group ($P=.0068$). The degree of atrial fibrosis quantified with Sirius red ($P=.0024$) showed that the proportion of fibrotic area was significantly greater in patients with AF than in those in SR (Fig. 1C and F).There was no microscopically or macroscopically visible thrombus in LA appendage in both groups. When we compare the clinical and histological findings in patients who were taking angiotensin receptor blocker (ARB)/angiotensin converting enzyme inhibitor (ACEi; $n=6$) and those without it ($n=26$), there was no significant difference in clinical characteristics and histological findings including SSM thickness, number of MFB, or

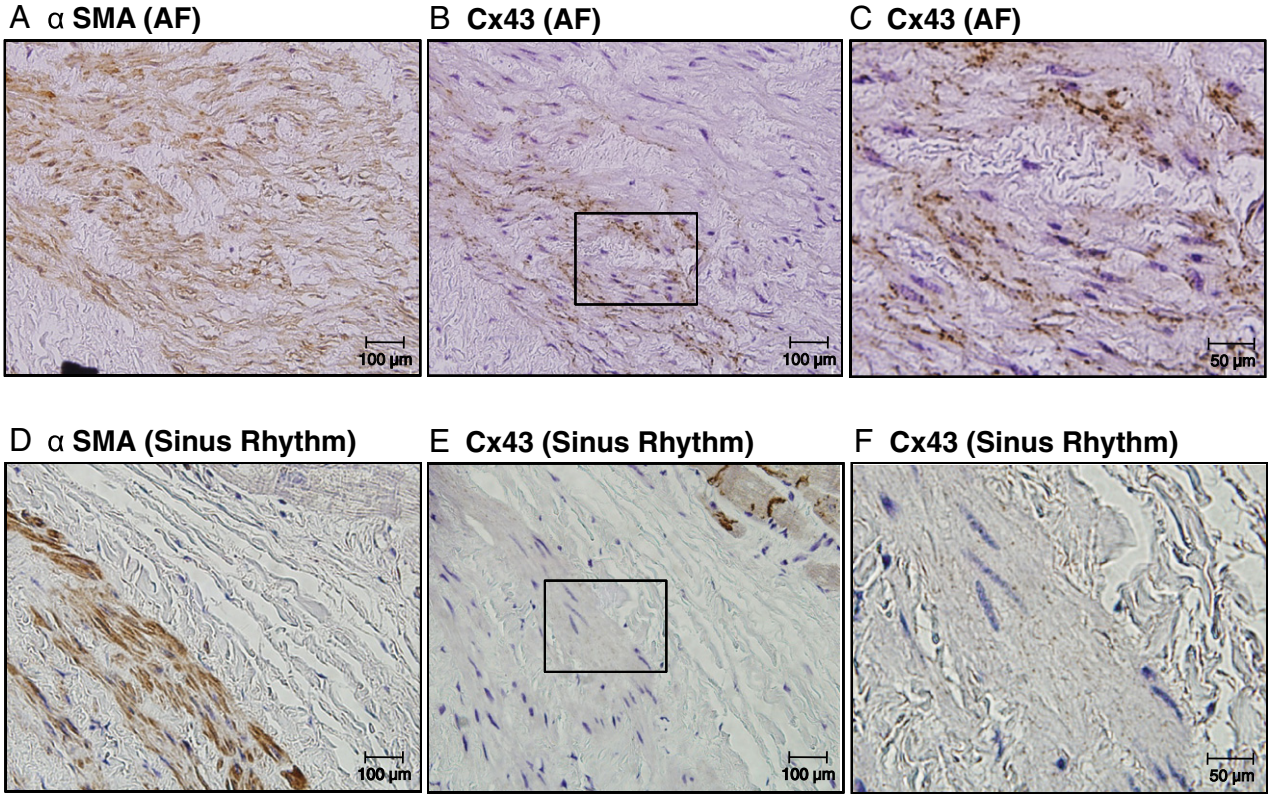

Fig. 2. Comparison of patients with AF (A–C) and SR (D–F) represented by α-SMA (A and D), Cx43 (400× magnifications, B and E), and Cx43 (1000× magnifications, C and F). We quantified the expression of Cx43 in the α-SMA-positive area.

degree of fibrosis, but left ventricular systolic (P=.0130) and diastolic dimensions (P=.0067) were greater in patients who were taking ARB/ACEi compared to those without it.

3.2. Thicker SSM layer in remodeled LA

We compared the clinical characteristics between the patients whose SSM layer ≥14 μm (n=20) and those whose layer <14 μm (n=20) depending on their median value (Table 3). The patients who had thicker SSM layer ≥14 μm had greater body mass index (P=.0133), LA size (P=.0006), and LA volume index (P=.0280), and higher proportion of mitral valve disease (P=.0460) than those with SSM layer <14 μm. In the quadrant analysis, SSM layer was weakly correlated to the LA size (R=0.5310, P=.0006; Fig. 3A) and fibrosis (R=0.5512, P=.0004; Fig. 3E). However, proportion of fibrosis area was not correlated to the LA size in this patient group with advance fibrosis (Fig. 3C). The thicker SSM group had a higher degree of atrial fibrosis measured in Sirius red stain (P=.0094). Among 17 patients with AF, we also compared clinical characteristic of the patients with SSM layer ≥40 μm (n=9) and those with SSM layer <40 μm (n=8) based on their median value (Table 4). AF patients with thick SSM layer have greater body mass index (BMI) (P=.0012) and LA remodeling (P=.0019) and higher degree of fibrosis (P=.004) than those with thin SSM thickness. In AF patients, the proportion of PAS (+) cells were also significantly higher in patients with thick SSM ≥40 μm than those with <40 μm (P=.0113; Table 4).

Table 2
Clinical and histological results in SR and AF patients

	SR (n=15)	AF (n=17)	p Value
Age	47.24±13.90	61.00±9.56	P=.0003
Sex (male)	11 (73.33%)	9 (52.94%)	P=.1100
BMI (kg/m^2)	22.47±2.91	21.65±3.45	P=.2278
BSA (m^2)	1.71±0.20	1.57±0.21	P=.0301
Mitral valve disease (%)	10 (58.82%)	23 (100.00%)	P=.0010
LA size (mm)	46.07±9.29	63.09±11.44	P<.0001
LA volume (ml)	96.79±42.20	185.35±98.95	P=.0012
LA volume index	61.22±20.67	126.39±59.43	P=.0024
LVEF (%)	58.24±11.32	63.87±12.19	P=.0724
E/E′	17.47±13.35 (n=6)	19.31±3.68 (n=9)	P=.3753
LVEDD	57.94±10.62	53.17±8.28	P=.0593
LVESD	40.71±10.14	35.57±8.41	P=.0440
Fibrosis (Sirius red) (% area)	27.10±7.83	37.55±12.06	P=.0024
Subendocardial smooth muscle (% area)	0.64±1.15	3.64±5.29	P=.0137
Subendocardial smooth muscle thickness (mm)	0.02±0.04	0.13±0.17	P=.0091
Endocardium thickness (mm)	0.14±0.21	0.37±0.31	P=.0068
Myofibroblast (n)	2.29±6.50	18.35±37.65	P=.0456
PAS (+) cells (%)	0.53±0.43	0.72±0.86	P=.2084

Table 3
Comparison of clinical and histological results according to SSM layer thickness

	SSM <14 μm (n=20)	SSM ≥14 μm (n=20)	P
AF	8 (40.00%)	15 (75.00%)	P=.0250
Age	54.70±13.82	55.60±13.21	P=.4172
Sex (male)	10 (50.00%)	10 (50.00%)	P=1.0000
BMI (kg/m^2)	21.07±3.37	23.46±2.66	P=.0133
BSA (m^2)	1.59±0.26	1.67±0.17	P=.1442
Mitral valve disease (%)	14 (70.00%)	19 (95.00%)	P=.0460
LA size (mm)	49.63±12.09	63.11±11.46	P=.0006
LA Volume (ml)	110.87±67.46	189.92±97.26	P=.0031
LA volume index	77.87±37.07	126.01±66.47	P=.0208
LVEF (%)	58.85±14.05	64.10±9.20	P=.0851
E/E′	18.50±12.22 (n=10)	17.62±6.32 (n=5)	P=.4419
LVEDD	56.90±11.66	53.50±6.64	P=.1320
LVESD	39.80±11.69	35.70±6.04	P=.0858
Fibrosis (Sirius red) (%)	28.76±8.42	37.53±12.90	P=.0094
Myofibroblast (n)	4.95±17.82	18.10±37.42	P=.0821
PAS (+) cells (%)	0.46±0.42	0.82±0.89	P=.0553

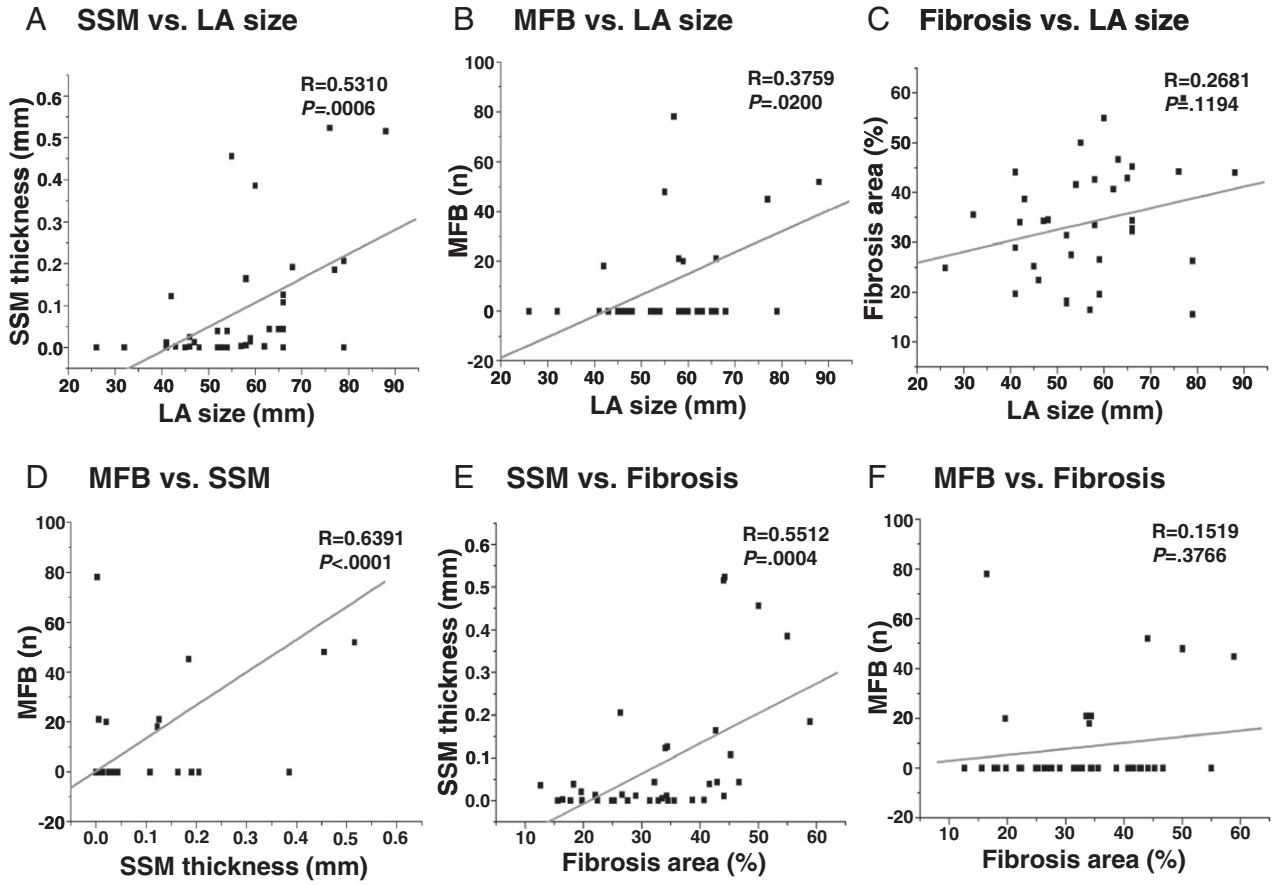

Fig. 3. Good correlation between the SSM layer thickness and LA size (A) and fibrosis (B). Fibrosis area was not correlated to the LA size (C). The number of MFBs and LA size (D), thickness of SSM layer and number of MFBs (E), and fibrosis area (F).

3.3. MFB does exist in human atrial tissue

Our definition of MFB was α-SMA-positive cells exhibiting disorganized patterns of Cx43 in Sirius red-stained fibrotic area (Fig. 2).We counted the number of nuclei in the spindle shaped cells in the area satisfying the definition of MFB immunostaining. MFBs were rarely found in SSM layer of fibrotic tissue, and they failed to be found in either the myocardial layer or epicardial layer. MFBs were found in seven out of 17 patients with AF (41.2%, Fig. 2A–C) and two out of 15 patients remaining in SR(13.3%, Fig. 2D–F). The number of MFBs tended to be greater in patients with AF [18.35±37.65 per tissue (a total of 422)] than in those in SR [2.29±6.50 per tissue (a total of 39), P=.0456]. We compared the areas where MFB was found to those with PAS-stained glycogen storage cells. Most of MFBs (95.5%) were colocalized with PAS stained glycogen storage cells (Fig. 4). The patients who showed MFBs in the atrial tissues had greater degree of LA structural remodeling (LA size 64.22±14.00 mm vs. 53.93±12.57 mm, P=.0218) and thicker SSM layer (0.22±0.22 vs. 0.04±0.08 mm, P=.0004) than those without MFB. The number of MFBs were weakly correlated to the LA size (R=0.3759, P=.0200; Fig. 3B) or thickness of SSM layer (R=0.6391, P<.0001; Fig. 3D) but not correlated with the proportion of fibrosis area in this patient group with significant structural heart disease (Fig. 3F).

Table 4
Comparison of clinical and histological results according to SSM layer thickness in patients with AF

	SSM <40 μm (n=8)	SSM ≥40 μm (n=9)	p Value
Age	56.25±12.19	61.67±7.42	P=.1397
Sex (Male)	4 (50.00%)	3 (33.33%)	P=.4860
BMI(kg/m^2)	18.66±3.07	23.18±1.98	P=.0012
BSA (m^2)	1.45±0.26	1.63±0.11	P=.0369
Mitral Valve Disease (%)	8 (100%)	9 (100%)	P=1.0000
LA size (mm)	53.38±8.09	68.67±10.07	P=.0019
LA volume (ml)	121.70±48.16	243.84±97.06	P=.0029
LA volume index	83.63±18.96	168.00±61.42	P=.0046
LVEF (%)	66.88±17.08	60.00±7.35	P=.1440
LVEDD	51.63±9.94	53.78±6.92	P=.3042
LVESD	33.75±12.14	37.78±5.74	P=.1932
Fibrosis (Sirius red) (%)	31.16±11.13	46.77±8.17	P=.0040
Myofibroblast (n)	12.25±27.47	33.67±52.20	P=.1580
PAS (+) cells (%)	0.29±0.15	1.35±1.17	P=.0113

4. Discussion

In this study, we demonstrated that the thickness of SSM layer in atrial tissue is closely related to AF and degrees of structural remodeling or fibrosis in patients who underwent open heart surgery. We also found that MFB does exist in the fibrotic SSM layer of atrial tissue with significant structural remodeling in patients with long-standing valvular AF. To the best of our knowledge, this is the first study documenting MFBs in human atrial tissues.

4.1. Atrial structural remodeling in AF

Atrial hemodynamic overload, such as that induced by diastolic dysfunction related to hypertension, diabetes, coronary artery disease, obesity [8], intensified neurohormonal activation by volume overload, or atriomyopathy [9], changes the electrophysiology of the atrium, resulting in AF. Increased LA pressure contributes to the AF initiation and maintenance [10], and LA ischemia reduces the conduction velocity, increasing LA's susceptibility to reentry [11]. In contrast, long-standing persistent AF itself induces atrial dilatation by

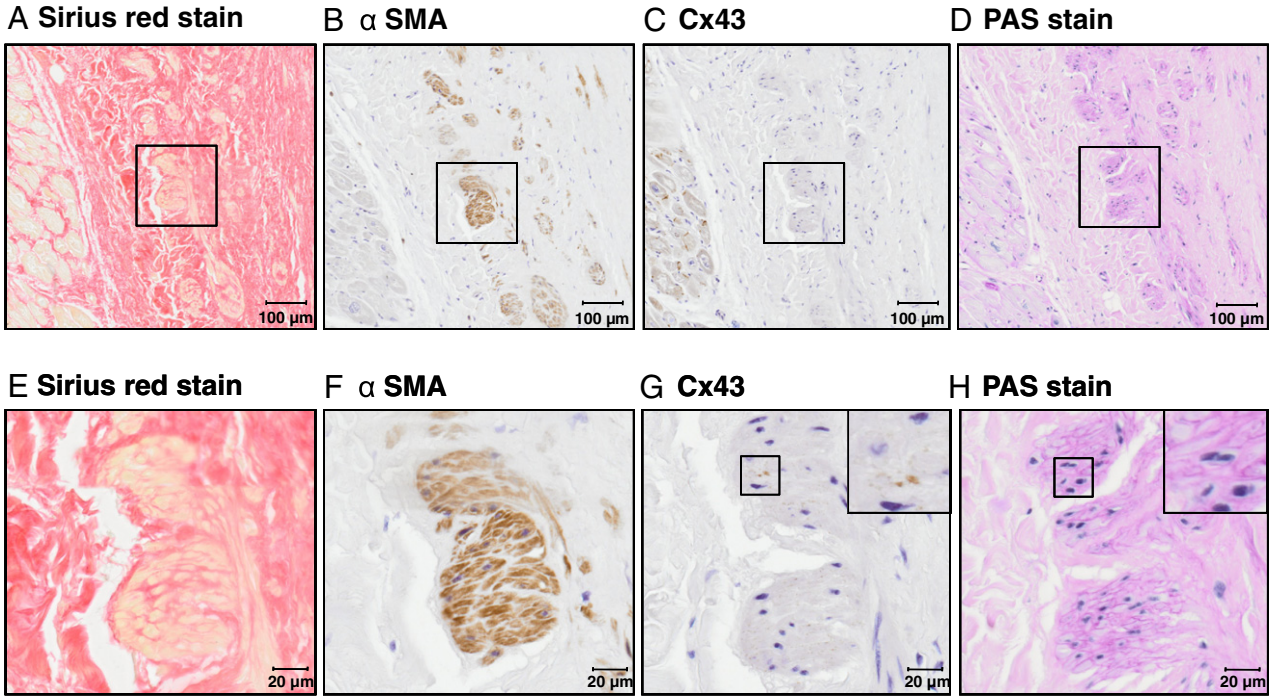

Fig. 4. In the same region, fibrotic areas stained with Sirius red stain (A), α-SMA (B), Cx43 (C) and PAS (marker for glycogen storage cells) (D) colocalized with MFBs. (E–H were magnified.)

changing LA function and increasing interstitial fibrosis [12]. We previously reported that morphologically remodeled atrium has a low endocardial voltage, different pattern of electrogram distribution, and the enlargement of the anterior portion of LA and that it is related to a higher recurrence rate after catheter ablation of AF [13,14]. The patients with remodeled LA showed a higher risk score and events of ischemic stroke [15]. The degree of electroanatomical remodeling of AF has been known to be related to myocardial fibrosis [16,17], matrix remodeling, and angiotensin II-nicotinamide adenine dinucleotide phosphate oxidase-mediated thrombus formation [18]. Therefore, there is a positive correlation between the amount of fibrosis and the persistence of AF [19], suggesting that AF itself causes structural remodeling that in turn promotes AF.

4.2. Roles of cardiac fibroblasts in histologically remodeled atrium

Cardiac fibroblasts make up only 10–15% of total cardiac cell volume, but 75% of cardiac cell number [20,21]. Cardiac fibroblasts are the source of extracellular matrix protein and conduct tissue fibrosis and remodeling. The extracellular matrix network has multiple functions that include the preservation of cell attachment, tissue architecture, and chamber geometry. In pathological conditions, such as ischemia, mechanical stretching, myocardial injury, reactive oxygen species, enhanced autocrine–paracrine mediator production, and inflammatory stimuli, cardiac fibroblasts proliferate, migrate, produce extracellular matrix proteins or cytokines, and differentiate into MFBs [22,23].The first description of MFBs was in the granulation tissue based on morphological techniques [24]. It was subsequently determined that tissues containing MFB contract in a similar fashion as smooth muscle, which facilitated the determination of their role in wound healing and the development of fibrosis. It has been reported that the atria are more susceptible to fibrosis than the ventricles, because of differential stretch and mechanical loading properties and the higher differentiation property of atrial fibroblasts than that of ventricular fibroblasts [2,25]. In this study, MFB was more frequently found in the atrial tissues taken from the patients with valvular AF, thicker SSM layer, and a higher degree of atrial fibrosis. Therefore, the thickened SSM layer may reflect reactive fibrosis or reparative fibrosis [26]. All MFBs we found existed in SSM layer with fibrosis. MFB may also be derived from cardiac endothelial cells [27] and from circulating precursors [28].

4.3. Potential roles of cardiac MFB in AF

The presence of fibrosis/low-voltage tissue has been postulated as a potential cause for abnormalities in atrial activation that may underlie the initiation and maintenance of fibrillation [29,30]. MFBs with their distinctive characteristic of greater expression of α-SMA may be coupled to myocytes via gap junction proteins Cx43 and Cx45 [31]. MFB expresses a variety of ion channels, in particular voltage-gated K channels, calcium-activated large conductance K^+ channels [32], and nonselective cation channels of the transient receptor potential (TRP) family [33]. Although fibroblasts appear to lack voltage-gated Ca^{2+} channels, TRP channels act as a gate for calcium entry and cell differentiation to extracellular matrix protein secretory phenotypes. Because MFBs have less negative resting membrane potential and slow depolarization and repolarization, and are electrically coupled with cardiomyocytes by gap junctions [7], it can generate arrhythmias by spontaneous impulse formation and reentry [34,35]. In this study, MFBs were well colocalized with the PAS-positive glycogen storage cells in LA appendage tissues. Nguyen et al. [36] also reported that PAS-positive cells stained positively form HCN4 and myoglobin, indicating potential pacemaking cells in human atrial tissue with AF. Lowered oxygen supply–demand ratio switches the energy metabolism of atrial cardiomyocyte from the use of fatty acids to the use of glucose, resulting in accumulation of glycogen and depleted contractile myofilaments [37]. Therefore, PAS stained cells colocalized with MFBs in our study may reflect as evidence of significant structural remodeling of AF.

4.4. Study limitations

Our study population was relatively small to compare the histological characteristics of valvular AF. Because of small sample

size and relatively homogeneous patient group associated long-standing valvular AF, we failed to demonstrate the clinical significance or functional importance of histologic characteristics in this study. Although pulmonary vein is a well-established trigger of AF, we did not perform histologic evaluation from LA-pulmonary vein junction but from LA appendage. However, LA appendage is an under-recognized trigger site of AF and non-pulmonary vein triggers are common in patients with longstanding persistent AF with significant atrial remodeling [38,39].We did not evaluate the functional implication of SSM in AF. Although we evaluated electrocardiography before and after the operation, pre-existing paroxysmal AF cannot be excluded in the SR group. Because the included patients had significant structural heart diseases requiring cardiac surgery, it is not a comparison with true control population of atrial appendage tissue and histological changes might have been partially induced by the effects of hemodynamic overload.

5. Conclusion

In this study, we demonstrated that the thickness of SSM layer in the atrial tissue is greater in patients with long-standing valvular AF than those in SR who underwent open heart surgery. The thickness of SSM was also related to the degree of atrial structural remodeling and fibrosis. MFBs were more frequently found in the fibrotic SSM layer of the patients with AF than those in SR, and well co-localized with glycogen storage cells.

Acknowledgments

This work was supported by a grant (A085136) from the Korea Health 21 R&D Project, Ministry of Health and Welfare, and a grant (2010-0010537) from the Basic Science Research Program run by the National Research Foundation of Korea (NRF), which is funded by the Ministry of Education, Science and Technology of the Republic of Korea.

References

[1] Tanaka K, Zlochiver S, Vikstrom KL, Yamazaki M, Moreno J, Klos M, Zaitsev AV, Vaidyanathan R, Auerbach DS, Landas S, Guiraudon G, Jalife J, Berenfeld O, Kalifa J. Spatial distribution of fibrosis governs fibrillation wave dynamics in the posterior left atrium during heart failure. Circ Res 2007;101(8):839–47.
[2] Li D, Fareh S, Leung TK, Nattel S. Promotion of atrial fibrillation by heart failure in dogs: atrial remodeling of a different sort. Circulation 1999;100(1):87–95.
[3] Manabe I, Shindo T, Nagai R. Gene expression in fibroblasts and fibrosis: involvement in cardiac hypertrophy. Circ Res 2002;91(12):1103–13.
[4] Weber KT. Fibrosis in hypertensive heart disease: focus on cardiac fibroblasts. J Hypertens 2004;22(1):47–50.
[5] Gabbiani G, Chaponnier C, Huttner I. Cytoplasmic filaments and gap junctions in epithelial cells and myofibroblasts during wound healing. J Cell Biol 1978;76(3):561–8.
[6] Spanakis SG, Petridou S, Masur SK. Functional gap junctions in corneal fibroblasts and myofibroblasts. Invest Ophthalmol Vis Sci 1998;39(8):1320–8.
[7] Rohr S. Myofibroblasts in diseased hearts: new players in cardiac arrhythmias? Heart Rhythm 2009;6(6):848–56.
[8] Tsang TS, Barnes ME, Gersh BJ, Bailey KR, Seward JB. Left atrial volume as a morphophysiologic expression of left ventricular diastolic dysfunction and relation to cardiovascular risk burden. Am J Cardiol 2002;90(12):1284–9.
[9] Pak HN, Hong SJ, Hwang GS, Lee HS, Park SW, Ahn JC, Moo Ro Y, Kim YH. Spatial dispersion of action potential duration restitution kinetics is associated with induction of ventricular tachycardia/fibrillation in humans. J Cardiovasc Electrophysiol 2004;15(12):1357–63.
[10] Li D, Melnyk P, Feng J, Wang Z, Petrecca K, Shrier A, Nattel S. Effects of experimental heart failure on atrial cellular and ionic electrophysiology. Circulation 2000;101(22):2631–8.
[11] Sinno H, Derakhchan K, Libersan D, Merhi Y, Leung TK, Nattel S. Atrial ischemia promotes atrial fibrillation in dogs. Circulation 2003;107(14):1930–6.
[12] Hoit BD, Shao Y, Gabel M, Walsh RA. Left atrial mechanical and biochemical adaptation to pacing induced heart failure. Cardiovasc Res 1995;29(4):469–74.
[13] Park JH, Pak HN, Choi EJ, Jang JK, Kim SK, Choi DH, Choi JI, Hwang C, Kim YH. The relationship between endocardial voltage and regional volume in electroanatomical remodeled left atria in patients with atrial fibrillation: comparison of three-dimensional computed tomographic images and voltage mapping. J CardiovascElectrophysiol 2009;20(12):1349–56.
[14] Park JH, Park SW, Kim JY, Kim SK, Jeoung B, Lee MH, Hwnag C, Kim Y-H, Kim SS, Pak HN. Characteristics of complex fractionated atrial electrogram in electroanatomically remodeled left atrium in patients with atrial fibrillation. Circ J 2010;74(8):1557–63.
[15] Park JH, Joung B, Son NH, Shim JM, Lee MH, Hwang C, Pak HN. The electroanatomical remodelling of the left atrium is related to CHADS2/CHA2DS2VASc score and events of stroke in patients with atrial fibrillation. Europace 2010;13(11):1541–9.
[16] Kostin S, Klein G, Szalay Z, Hein S, Bauer EP, Schaper J. Structural correlate of atrial fibrillation in human patients. Cardiovasc Res 2002;54(2):361–79.
[17] Nakai T, Chandy J, Nakai K, Bellows WH, Flachsbart K, Lee RJ, Leung JM. Histologic assessment of right atrial appendage myocardium in patients with atrial fibrillation after coronary artery bypass graft surgery. Cardiology 2007;108(2):90–6.
[18] Goette A, Bukowska A, Lendeckel U, Erxleben M, Hammwohner M, Strugala D, Pfeiffenberger J, Rohl FW, Huth C, Ebert MP, Klein HU, Rocken C. Angiotensin II receptor blockade reduces tachycardia-induced atrial adhesion molecule expression. Circulation 2008;117(6):732–42.
[19] Boldt A, Wetzel U, Lauschke J, Weigl J, Gummert J, Hindricks G, Kottkamp H, Dhein S. Fibrosis in left atrial tissue of patients with atrial fibrillation with and without underlying mitral valve disease. Heart 2004;90(4):400–5.
[20] McAnulty RJ, Laurent GJ. Collagen synthesis and degradation in vivo. Evidence for rapid rates of collagen turnover with extensive degradation of newly synthesized collagen in tissues of the adult rat. Coll Relat Res 1987;7(2):93–104.
[21] Banerjee I, Fuseler JW, Price RL, Borg TK, Baudino TA. Determination of cell types and numbers during cardiac development in the neonatal and adult rat and mouse. Am J Physiol Heart Circ Physiol 2007;293(3):H1883–91.
[22] Swynghedauw B. Molecular mechanisms of myocardial remodeling. Physiol Rev 1999;79(1):215–62.
[23] Weber KT, Sun Y, Tyagi SC, Cleutjens JP. Collagen network of the myocardium: function, structural remodeling and regulatory mechanisms. J Mol Cell Cardiol 1994;26(3):279–92.
[24] Gabbiani G, Ryan GB, Majne G. Presence of modified fibroblasts in granulation tissue and their possible role in wound contraction. Experientia 1971;27(5):549–50.
[25] Burstein B, Libby E, Calderone A, Nattel S. Differential behaviors of atrial versus ventricular fibroblasts: a potential role for platelet-derived growth factor in atrial-ventricular remodeling differences. Circulation 2008;117(13):1630–41.
[26] Yue L, Xie J, Nattel S. Molecular determinants of cardiac fibroblast electrical function and therapeutic implications for atrial fibrillation. Cardiovasc Res 2011;89(4):744–53.
[27] Goumans MJ, van Zonneveld AJ, ten Dijke P. Transforming growth factor beta-induced endothelial-to-mesenchymaltransition: a switch to cardiac fibrosis? Trends Cardiovasc Med 2008;18(8):293–8.
[28] van Amerongen MJ, Bou-Gharios G, Popa E, van Ark J, Petersen AH, van Dam GM, van Luyn MJ, Harmsen MC. Bone marrow-derived myofibroblasts contribute functionally to scar formation after myocardial infarction. J Pathol 2008;214(3):377–86.
[29] Spach MS, Boineau JP. Microfibrosis produces electrical load variations due to loss of side-to-side cell connections: a major mechanism of structural heart disease arrhythmias. Pacing Clin Electrophysiol 1997;20(2 Pt 2):397–413.
[30] Spach MS, Josephson ME. Initiating reentry: the role of nonuniform anisotropy in small circuits. J Cardiovasc Electrophysiol 1994;5(2):182–209.
[31] Camelliti P, Devlin GP, Matthews KG, Kohl P, Green CR. Spatially and temporally distinct expression of fibroblast connexins after sheep ventricular infarction. Cardiovasc Res 2004;62(2):415–25.
[32] Wang YJ, Sung RJ, Lin MW, Wu SN. Contribution of BK(Ca)-channel activity in human cardiac fibroblasts to electrical coupling of cardiomyocytes-fibroblasts. J Membr Biol 2006;213(3):175–85.
[33] Runnels LW, Yue L, Clapham DE. The TRPM7 channel is inactivated by PIP(2) hydrolysis. Nat Cell Biol 2002;4(5):329–36.
[34] Zlochiver S, Munoz V, Vikstrom KL, Taffet SM, Berenfeld O, Jalife J. Electrotonic-myofibroblast-to-myocyte coupling increases propensity to reentrant arrhythmias in two-dimensional cardiac monolayers. Biophys J 2008;95(9):4469–80.
[35] Jacquemet V, Henriquez CS. Modelling cardiac fibroblasts: interactions with myocytes and their impact on impulse propagation. Europace 2007;9(Suppl. 6):vi29–37.
[36] Nguyen BL, Fishbein MC, Chen LS, Chen PS, Masroor S. Histopathological substrate for chronic atrial fibrillation in humans. Heart Rhythm 2009;6(4):454–60.
[37] Ausma J, Wijffels M, Thone F, Wouters L, Allessie M, Borgers M. Structural changes of atrial myocardium due to sustained atrial fibrillation in the goat. Circulation 1997;96(9):3157–63.
[38] Pak HN, Hwang C, Lim HE, Kim JW, Lee HS, Kim YH. Electroanatomic characteristics of atrial premature beats triggering atrial fibrillation in patients with persistent versus paroxysmal atrial fibrillation. J CardiovascElectrophysiol 2006;17(8):818–24.
[39] Di Biase L, Burkhardt JD, Mohanty P, Sanchez J, Mohanty S, Horton R, Gallinghouse GJ, Bailey SM, Zagrodzky JD, Santangeli P, Hao S, Hongo R, Beheiry S, Themistoclakis S, Bonso A, Rossillo A, Corrado A, Raviele A, Al-Ahmad A, Wang P, Cummings JE, Schweikert RA, Pelargonio G, Dello Russo A, Casella M, Santarelli P, Lewis WR, Natale A. Left atrial appendage: an underrecognized trigger site of atrial fibrillation. Circulation 122(2):109–18.